THE JOURNAL OF PHYSICAL CHEMISTRY Letters

pubs.acs.org/JPCL Letter

Toward Quantitative Prediction of Fluorescence Quantum Efficiency by Combining Direct Vibrational Conversion and Surface Crossing: BODIPYs as an Example

Qi Ou, Qian Peng, and Zhigang Shuai*

Cite This: J. Phys. Chem. Lett. 2020, 11, 7790−7797 Read Online

ACCESS | Metrics & More | Article Recommendations | Supporting Information

ABSTRACT: Accurate theoretical description of the electronic structure of boron dipyrromethene (BODIPY) molecules has been a challenge, let alone the prediction of fluorescence quantum efficiency. In this Letter, we show that the electronic structures of BODIPYs can be accurately evaluated via the spin-flip time-dependent density functional theory with the B3LYP functional. With the resulting electronic structures, the experimental spectral line shapes of representative BODIPYs are successfully reproduced by our previously developed thermal vibration correlation function method. Most importantly, a two-channel scheme is proposed to describe the internal conversion of S_1 to S_0 in BODIPYs: channel I via direct vibrational relaxation within the harmonic region and channel II via a distorted S_0/S_1 minimum energy crossing point well away from the harmonic region. The fluorescence quantum yields are accurately predicted within this two-channel scheme, which can therefore serve as a generalized method for predicting the photophysical parameters of organic fluorescent compounds.

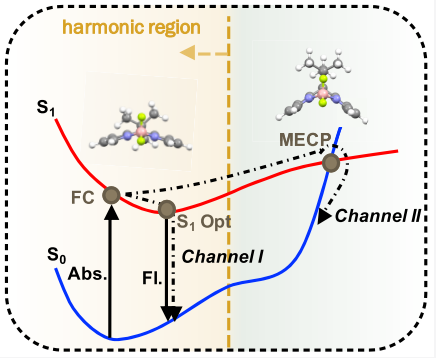

Recently, boron dipyrromethene derivatives (BODIPYs) have become a cutting-edge topic in the field of dye chemistry due to their distinguished photophysical properties, including intense fluorescence with narrow peaks and high quantum yields, high extinction coefficients, and tunable emission wavelength via extensive substitution variations.[1−7] Given the remarkable experimental significance of BODIPYs, a number of theoretical and computational efforts have been devoted to unraveling their extraordinary photophysical properties.[8−13] Nevertheless, the conventional time-dependent density functional theory (TDDFT), which serves as the method of choice for most organic compounds, always severely overestimates the energy of the light-emitting state (S_1) of BODIPYs because of its presumable double-excitation and/or multireference nature.[11,12,14−17] In addition, a reliable description of the decay process of S_1 is desired to enable better exploration of the photophysical property and quantitative prediction of the fluorescence quantum efficiency via the equation $\Phi_{fl} = k_r/(k_r + k_{nr})$, where k_r and k_{nr} correspond to the radiative and nonradiative decay rate constants, respectively. This has been a long-standing challenge for theoretical chemistry because the radiative decay is usually on the order of 10 ns, which is 3 orders of magnitude longer than the typical time span of the best currently available excited state dynamics simulation.[18−20] The nonradiative decay rate constant k_{nr} of most organic fluorophores spans a much wider scale: for a strongly fluorescent compound, k_{nr} can be orders of magnitude smaller, while it can be much larger for weakly luminescent compounds. Therefore, a rate formalism such as the thermal vibration correlation function (TVCF) has become the practical approach for quantitatively predicting Φ_{fl}, by which the nonradiative decay is modeled as a vibrational relaxation-induced nonadiabatic transition (channel I in Figure 1).[21] Coupled with quantum chemistry calculations, TVCF has found great success in improving our quantitative understanding of photophysical phenomena such as aggregation-induced emission.[22] Recently, Lin et al. proposed a data-driven, semiempirical scheme for assessing the nonradiative decay rate of BODIPY molecules via the access of a S_0/S_1 minimum energy crossing point (MECP) (channel II in Figure 1), by which Φ_{fl} can be efficiently predicted according to a combination of inexpensive quantum chemical calculations and experimental spectroscopic data.[11] However, the predicted results based on such an algorithm depend on the choice of the "training set", and channel I is completely ignored within this algorithm.

From the perspective of electronic structure theory, to tackle the problem encountered by conventional TDDFT in BODIPYs, on one hand, highly accurate correlated wave

Received: July 4, 2020
Accepted: August 7, 2020
Published: August 7, 2020

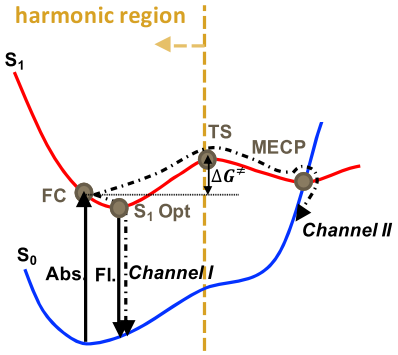

Figure 1. Schematic graph of two internal conversion channels of S_1. FC is the Franck−Condon point. S_1 Opt is the S_1 optimized structure. TS is the transition state. Solid arrows indicate radiative transitions with a photon being absorbed or emitted. Dashed−dotted lines indicate nonradiative processes. Channel I corresponds to the decay channel via direct harmonic vibrational relaxation; channel II corresponds to the decay channel via a distorted S_0/S_1 MECP structure.

function methods such as coupled-cluster theory[10,14,15,23] and multireference approaches[14,24−30] have been applied to gain a more reliable description, sacrificing computational efficiency as compared with TDDFT. On the other hand, data-driven models based on a linear fitting between experimental excitation energies and TDDFT-predicted results have been proposed to efficiently correct the original overestimation.[11,14,31−33] While such a linear regression approach has found success in predicting the excitation energies,[14,31−33] its accuracy depends on the choice of the "training set" within the fitting model. Therefore, an efficient yet robust *ab initio* approach is still desired for BODIPYs, with the availability of the corresponding electronic structure quantities (i.e., analytical gradient, nonadiabatic coupling, etc.) required by further evaluation of photophysical properties.

Bearing the aforementioned obstacles in mind, we demonstrate in this Letter that the spin-flip version of TDDFT (SF-TDDFT), which is able to capture double-excitation and multireference character with nearly the same computational cost as conventional TDDFT,[34] can serve as a golden method for describing the electronic structures of BODIPY families. Among all previous theoretical studies of BODIPY systems, to the best of our knowledge, SF-TDDFT has been applied by Lin et al. only to locate the S_0/S_1 MECP, while they returned to conventional TDDFT to calculate the excitation energies and transition dipole moments according to ref 11. Most importantly, we propose a general computational protocol for describing the nonradiative decay of S_1 through combination of the two channels (in Figure 1), with the TVCF formalism applied to channel I and transition state theory (TST) applied to channel II. On the basis of this two-channel scheme, the fluorescence quantum efficiency of BODIPY molecules can be accurately predicted without any fitting parameter, and this computational protocol can be easily generalized to other organic fluorophores with complex structures.

The investigated BODIPY molecules are listed in Scheme 1. The S_0 and S_1 states are optimized via SF-TDDFT using the B3LYP functional and cc-pVDZ basis set in quantum chemistry package Q-Chem 5.2,[35] with solvent effects addressed via linear-response polarized continuum model LR-PCM.[36−38] While the BHHLYP functional is considered

Scheme 1. Chemical Structures of the Investigated BODIPYs

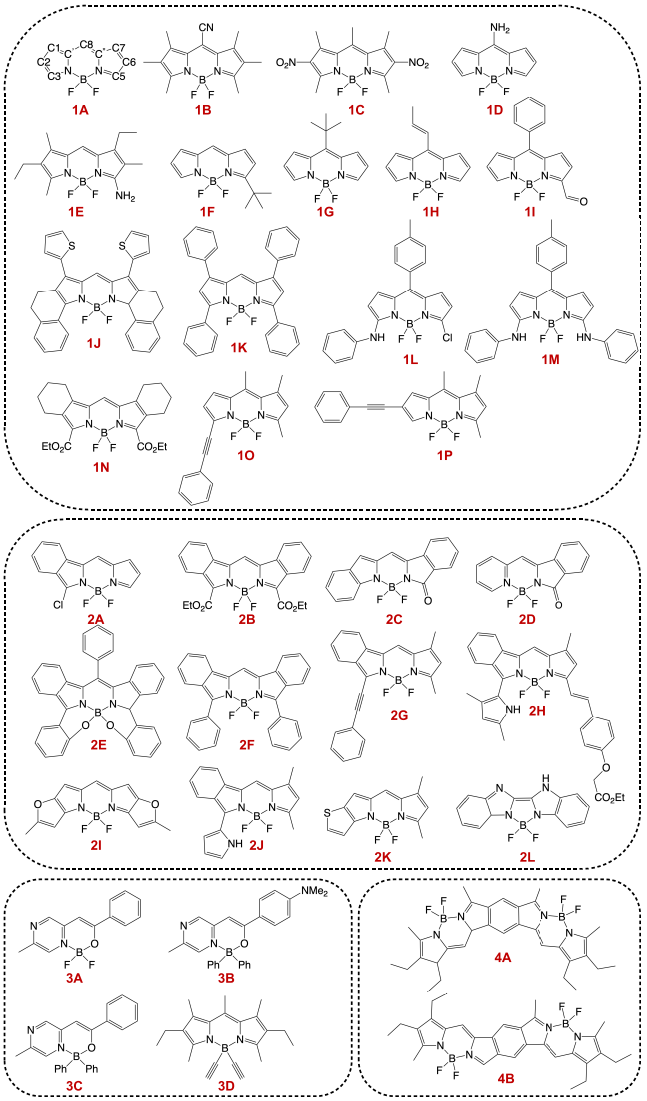

as a successful functional for SF-TDDFT as previously reported,[39] we have found that this functional does not offer reliable predictions for BODIPY excitation energies, accompanied with a serious spin contamination issue (see the computed vertical excitation energies and the $\langle S^2 \rangle$ values for BODIPY **1A** in Table S1). Therefore, the B3LYP functional is applied throughout this study, which can be justified by the following computational results.

The computational vertical excitation energies at S_0 and S_1 geometries, namely, the theoretical absorption and emission energies, respectively, are plotted in Figure 2 with a comparison of the corresponding experimental values. Explicit numbers as well as the type of solvents for each investigated BODIPY are listed in Tables S2 and S3. Even though a contradictory argument has arisen with regard to the rationality of such a comparison for BODIPYs,[12,40] it serves as a reasonable protocol and even as the rule of thumb for judging the accuracy of the applied electronic structure theory in most theoretical works,[41−43] and we find BODIPYs are not the exception. For the sake of rigorousness, a well-grounded comparison of the computed 0−0 energies versus the

https://dx.doi.org/10.1021/acs.jpclett.0c02054
J. Phys. Chem. Lett. 2020, 11, 7790−7797

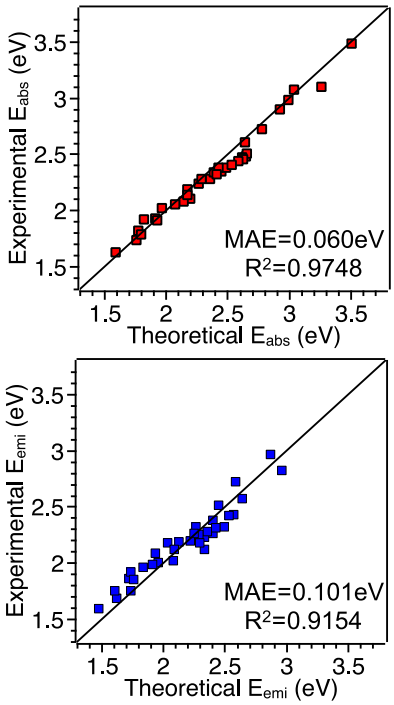

Figure 2. Comparison between theoretical (SF-TDDFT/B3LYP/cc-pVDZ with LR-PCM) vertical excitation energies and experimental absorption (top) and fluorescence (bottom) maxima.

experimental absorption/fluorescence crossing point (AFCP) will be carried out next.

Figure 2 shows that vertical excitation energies predicted by SF-TDDFT/B3LYP/cc-pVDZ with LR-PCM are in remarkably good agreement with experimental results. Contrary to a severe overestimation of the conventional TDDFT method, the mean absolute errors (MAEs) for absorption and emission energies predicted by SF-TDDFT are 0.060 and 0.101 eV, respectively, with linear fitting coefficients R^2 of >0.91. Such accurate and precise computational results over a wide range of BODIPY molecules rely on the fact that SF-TDDFT treats both S_0 and S_1 states as a linear combination of configurations generated via applying a spin-flip ($M_S = -1$) operator on top of the high-spin ($M_S = 1$) triplet reference state, in which the double-excitation configuration is effectively involved.[34] Therefore, the double-excitation and/or multiconfiguration character of BODIPY molecules, which has been previously revealed by multireference methods,[14,24] can be appropriately addressed within the SF-TDDFT framework. The computed transition dipole moment for BODIPY **1A** given by SF-TDDFT is also closer to the value given by correlated wave function method ADC(2) than the one given by conventional TDDFT (see Table S4). Furthermore, the well-known spin contamination issue associated with SF-TDDFT/B3LYP is not severe for all tested BODIPY systems according to the $\langle S^2 \rangle$ values of states S_0 and S_1 as listed in Tables S2 and S3.

The optimized ground state structure of BODIPYs is checked by comparing the computational results with the experimentally available structure obtained via X-ray diffraction (XRD). For BODIPY **1A**, the SF-TDDFT/B3LYP/cc-pVDZ-optimized structure is compared with the previously reported XRD experimental structure and CASPT2/6-31G* results (ref 25) in Table 1. Despite the modest influence of different basis sets, the SF-TDDFT-optimized structure generates results as

Table 1. Key Geometrical Parameters of BODIPY 1A Obtained from This Work, the CASPT2 Method, and XRD Experiments[a]

	this work[b]	CASPT2 6-31G*[c]	XRD experiments[c]
	Bonds (Å)		
B−F	1.408	1.388	1.405
B−N	1.557	1.561	1.545
N−C3	1.342	1.352	1.339
C3−C2	1.414	1.406	1.400
C2−C1	1.395	1.390	1.370
C1−C′	1.417	1.425	1.410
C′−C8	1.395	1.385	1.383
C′-N	1.403	1.389	1.391
	Angles (deg)		
F−B−F	109.6	111.8	108.6
N−B−N	106.5	104.9	106.6
C′−C8−C″	121.6	121.7	123.3
N−C′−C8	120.4	121.3	118.9
B−N−C′−C8	6.6	0	4.3

[a]Corresponding atoms indices are labeled in the chemical structure of **1A** in Scheme 1. [b]Ground state structure listed in Table 1 obtained via single-molecule optimization with no PCM applied. [c]Data obtained from ref 25.

good as those of CASPT2 and perfectly reproduces the key geometrical parameters of **1A**, including a small B−N−C′−C8 dihedral angle that is missing in the CASPT2 calculation. Additionally, the visualized computational and experimental structures of BODIPYs **1G**, **1I**, **2C**, **2D**, and **2K** are compared in Figure S1, and only trivial deviations are observed between the computational and experimental structures for all tested cases.

As opposed to vertical excitation energies, 0−0 energies are well-defined via the energy gap between zeroth vibrational states and are directly comparable with experimental AFCP energies.[44−46] For BODIPY families, 0−0 energies (as well as spectral line shapes) have been theoretically explored by Chibani et al. via conventional TDDFT methods.[12] According to their results, the overestimation problem of TDDFT for BODIPY systems still exists for 0−0 energies: the MAE of predicted 0−0 energies compared to experimental AFCP values is as large as 0.374 eV.[12] Here we revisit this problem via the SF-TDDFT method for representative BODIPYs. Note that a vibrational analysis is required to obtain the zero-point vibrational energy (ZPVE), which is extremely time-consuming without the implementation of an analytical Hessian. Therefore, BODIPYs with 40 or fewer atoms listed in Scheme 1 are chosen as representatives. The same choice applies to the computation of fluorescence quantum efficiency.

The 0−0 energies of 13 representative BODIPYs predicted by SF-TDDFT are plotted in Figure 3 with respect to the corresponding experimental AFCP values. Explicit numbers and molecules can be found in Table S5. One can see from Figure 3 and Table S5 that the MAEs of predicted 0−0 energies are further decreased compared to the MAEs of vertical excitation energies. The high precision remains as indicated by an R^2 of 0.9490. The rationality of our applied electronic structure method is thus highlighted to a greater extent.

With the predicted 0−0 energies and vibrational analysis, the absorption/emission spectra of the 13 representative BODIPYs can be determined via the TVCF method in our self-developed

https://dx.doi.org/10.1021/acs.jpclett.0c02054
J. Phys. Chem. Lett. 2020, 11, 7790−7797

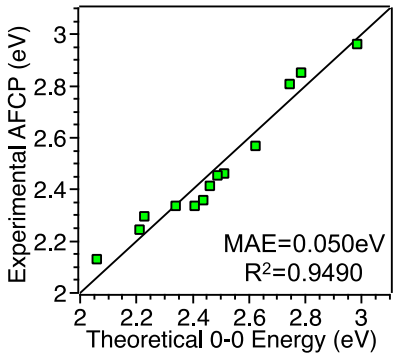

Figure 3. Comparison between theoretical (SF-TDDFT/B3LYP/cc-pVDZ with LR-PCM) 0−0 energies and experimental AFCP values.

molecular material property prediction package MOMAP 2019B.[22,47,48] The absorption and emission spectra are given as[49]

$$\sigma_{abs}(\omega) = \frac{4\pi^2\omega}{3c} \sum_{v_i,v_f} P_{iv_i}(T)|\langle\Theta_{fv_f}|\vec{\mu}_{fi}|\Theta_{iv_i}\rangle|^2\delta(\hbar\omega - E_{fi} - E_{fv_f} + E_{iv_i}) \quad (1)$$

$$\sigma_{em}(\omega) = \frac{4\omega^3}{3c^3} \sum_{v_i,v_f} P_{iv_i}(T)|\langle\Theta_{fv_f}|\vec{\mu}_{fi}|\Theta_{iv_i}\rangle|^2\delta(E_{if} + E_{iv_i} - E_{fv_f} - \hbar\omega) \quad (2)$$

where $P_{iv_i}(T)$ is the Boltzmann distribution function for the initial vibronic manifold, Θ_{iv_i} and Θ_{fv_f} are vibrational wave functions, E_{fi} (E_{if}) is the adiabatic energy gap between the final (initial) and initial (final) electronic states, and E_{iv_i} and E_{fv_f} are vibrational energies in the corresponding electronic states. Computational spectra of selected molecules (**1A**, **2C**, and **2D**) are shown in Figure 4, and results for other molecules are shown in Figure S2. We list the absorption and fluorescence maxima of both theoretical and experimental results in Table S6 for an easier comparison. One can see in Figure 4a and Table S6 that for BODIPY **1A**, the main peaks as well as the characteristic shoulders on both absorption and emission spectra are accurately captured, with an extremely small Stokes shift and a narrow full width at half-maximum (fwhm), in good agreement with experimental results in ref 50. Similar line shapes for **1A** have been obtained by Chibani et al. using a convoluting Gaussian function method with the electronic structure information obtained from conventional TDDFT, though the locations of the main peaks are severely blue-shifted due to the overestimation of the 0−0 energy by TDDFT.[12]

For BODIPYs **2C** and **2D**, multiple main peaks shown in absorption spectra are correctly reproduced as shown in panels b and c of Figure 4, with rational relative intensities compared to the experimental results from ref 51. Again, similar absorption spectral line shapes have been reported in ref 12, though with blue-shifted main peaks. For fluorescence spectra of BODIPYs **2C** and **2D**, the locations of each main peak are also correctly captured, while the relative intensities slightly deviate from those from the experiments: the theoretically predicted 0−0 transition is more intense than the 0−1 transition for these two molecules, which is contrary to the experimental fluorescence spectra. Such a mismatch of the relative intensities possibly resulted from practically rather complex molecular vibrational motions, which cannot be intuitively addressed within the current theoretical framework. Nevertheless, both absorption and fluorescence spectral line shapes of most investigated molecules are in perfect agreement with the experimental results (see Figure S2 and Table S6), and therefore, the adaptability of the SF-TDDFT method combining the TVCF approach soundly holds for predicting the spectra of BODIPY systems.

The computation of fluorescence quantum efficiency Φ_{fl} for BODIPY systems is undoubtedly crucial for practical application and rational molecular design. While the work of Lin et al.[11] is of great significance for qualitatively determining the Φ_{fl} of medium and large BODIPYs based on a combination of inexpensive quantum chemical calculations and experimental spectroscopic data, we evaluate Φ_{fl} from a non-empirical perspective that does not rely on any experimental results, which aims to unravel more physical insights but with a much higher computational cost compared to that of Lin et al.

To compute Φ_{fl} values for 13 representative BODIPYs, we first evaluate the k_r and k_{nr} of the S_1 state via the TVCF method based on the electronic structure information obtained via SF-TDDFT. The radiative rate of S_1 can be evaluated via TVCF formalism as[49]

$$k_r^{TVCF} = \int_0^\infty \sigma_{em}(\omega)\, d\omega \quad (3)$$

The normal nonradiative decay process of S_1 consists of two components, i.e., internal conversion (IC) to S_0 and intersystem crossing (ISC) to T_1. For 13 representative BODIPY molecules, no significant S_1−T_1 ISC processes have been reported experimentally to the best of our knowledge, and according to the El-Sayed rule,[52] the S_1−T_1 spin−orbit coupling (SOC) is expected to be negligible due to the almost identical transition character of S_1 and T_1 predicted by SF-TDDFT for all 13 molecules (Table S7). The large adiabatic energy gap between S_1 and T_1 (Table S7) will also limit ISC. Therefore, we neglect ISC of S_1 and approximate nonradiative rate constant k_{nr} of S_1 as IC rate constant k_{ic}. The TVCF

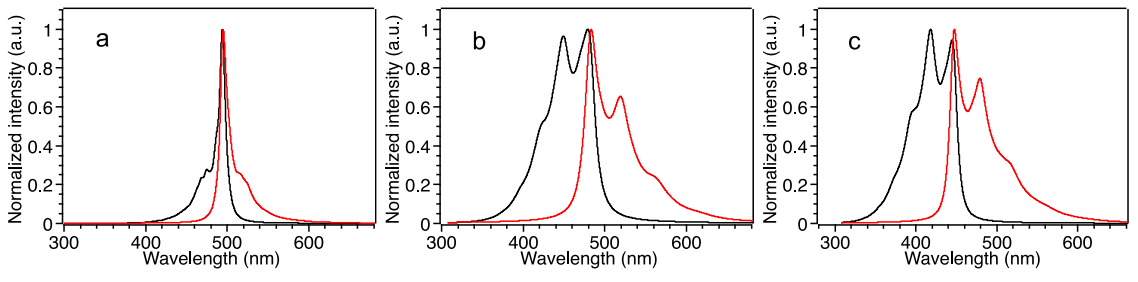

Figure 4. Theoretical absorption (black) and fluorescence (red) spectra of BODIPYs (a) **1A**, (b) **2C**, and (c) **2D**.

https://dx.doi.org/10.1021/acs.jpclett.0c02054
J. Phys. Chem. Lett. 2020, 11, 7790−7797

Table 2. Computational Rate Constants k_r^{TVCF} and k_{nr}^{TVCF} and Fluorescence Quantum Efficiencies Φ_{fl}^{cal} of 13 Representative BODIPYs[a]

molecule	k_r^{TVCF} ($\times 10^8$ s^{-1})	k_{nr}^{TVCF} ($\times 10^8$ s^{-1})	Φ_{fl}^{cal}	Φ_{fl}^{exp}	error %	solvent	ref
1A	1.90	0.32	0.86	0.92	6.5	ethanol	50
1C	2.67	4.44	0.38	0.31	22.6	methanol	54
1D	2.20	0.11	0.95	0.92	3.0	methanol	55
1F	2.18	0.36	0.86	1.00	14.0	methanol	26
1G	1.17	3.73	0.24	0.04	500.0	methanol	26
1H	1.12	3.09	0.27	0.05	440.0	THF	56
1I	1.65	3.29	0.33	0.29	13.8	dichloromethane	57
2A	1.87	0.52	0.78	0.62	25.8	dichloromethane	58
2C	2.32	2.12	0.52	0.49	6.1	dichloromethane	51
2D	2.59	1.60	0.62	0.47	31.9	dichloromethane	51
2I	2.52	0.56	0.82	0.96	14.6	chloroform	59
2K	2.07	4.35	0.32	0.34	5.8	chloroform	60
3A	2.30	2.17	0.51	0.57	10.5	dichloromethane	61

[a]Experimental fluorescence quantum efficiencies Φ_{fl}^{exp} and solvents are also listed for comparison.

method is first employed, and the nonradiative decay rate constant of S_1 is evaluated as[49]

$$k_{nr}^{TVCF} = \frac{1}{\hbar^2}\sum_{kl} R_{fi,kl}\int_{-\infty}^{\infty} dt Z_i^{-1} e^{i\omega_{if}t}\rho_{fi,kl}(t, T) \quad (4)$$

With

$$\rho_{fi,kl}(t, T) = \mathrm{Tr}(\hat{P}_{fk} e^{-i\tau_f \hat{H}_f}\hat{P}_{fl} e^{-i\tau_i \hat{H}_i}) \quad (5)$$

corresponding to the IC TVCF and

$$R_{fi,kl} = \langle\Theta_f|\hat{P}_{fk}|\Theta_i\rangle\langle\Theta_i|\hat{P}_{fl}|\Theta_f\rangle \quad (6)$$

where $\hat{P}$ is the nuclear momentum operator and Z_i is the partition function for the initial state parabola. The TVCF-evaluated k_r and k_{nr} values and the resulting Φ_{fl} values are listed in Table 2, together with the experimental Φ_{fl} values for reference. One can see in Table 2 that the TVCF-predicted Φ_{fl} values for most molecules are in good agreement with the experimental values. Nevertheless, two large percentage errors are found in two BODIPYs (**1G** and **1H**) with extremely low efficiency compared to those of other molecules. The low efficiencies of these two molecules have been experimentally and theoretically investigated.[12,26,53] On the basis of previous studies, this weakly fluorescent character can be attributed to a significant rotation of the 8 position substituent of the BODIPY ring (see the labeling of molecule **1A** in Scheme 1) and a resulting low-lying S_0/S_1 MECP, which opens an extremely efficient nonradiative decay channel.

To reinvestigate this problem within our current framework and quantitatively predict Φ_{fl} for **1G** and **1H**, we first plot the mode-specific reorganization energies of **1G** and **1H** in Figure 5 (while the same plots for other representative BODIPYs are shown in Figure S3). Clearly, in Figure 5 and Figure S3, most investigated BODIPY molecules show insignificant reorganization energy contributions from low-frequency vibrational modes except for **1G** and **1H**. The major contributing low-frequency modes (with Huang-Rhy's factor being >1.0) of **1G** and **1H** are visualized in Figure 5. For both molecules, large Huang-Rhy's factors arise from the rotation of the 8 position substituent as well as the wiggling of two pyrrole rings. Compared to the ground state geometry, the S_1-optimized geometries of **1G** and **1H** show salient distortion from planarity, accompanied by a pronounced rotation of the 8 position substituent [*tert*-butyl for **1G** and propenyl for **1H**

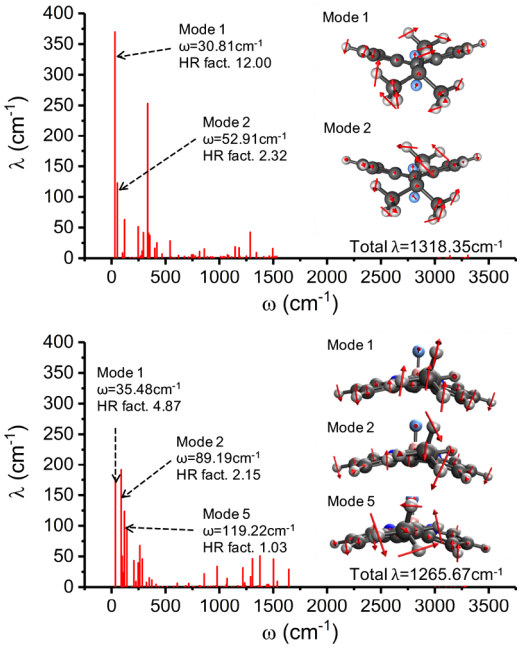

Figure 5. Decomposition of the reorganization energies of BODIPYs **1G** (top) and **1H** (bottom). For both molecules, low-frequency vibrational modes with Huang-Rhy's (HR) factors of >1.00 are visualized in the insets.

(shown in Figure S4)]. The significant deviation of the S_1 structure from the ground state geometry leads to a large total reorganization energy (with a major contribution from the low-frequency modes) and a broadened spectral line shape compared to other BODIPY molecules (Figure S2). Moreover, low-lying S_0/S_1 MECPs have been located via the penalty function method proposed by Levine et al.[62] in Q-Chem for both molecules (with the structure and relative energies shown in Figure S4), which are crucial to the fast radiationless decay processes. The MECP structure of **1G** located in this work is almost identical to the MECP structure predicted by CASPT2 in ref 26, which again emphasizes the equally good performance of SF-TDDFT compared to CASPT2.

Within our proposed two-channel IC scheme, the total k_{nr} for these two molecules should be computed as $k_{nr} = k_{nr}^{TVCF} + k_{nr}^{MECP}$, where k_{nr}^{TVCF} and k_{nr}^{MECP} correspond to the nonradiative decay rate constants of two deactivation channels. To

https://dx.doi.org/10.1021/acs.jpclett.0c02054
J. Phys. Chem. Lett. 2020, 11, 7790−7797

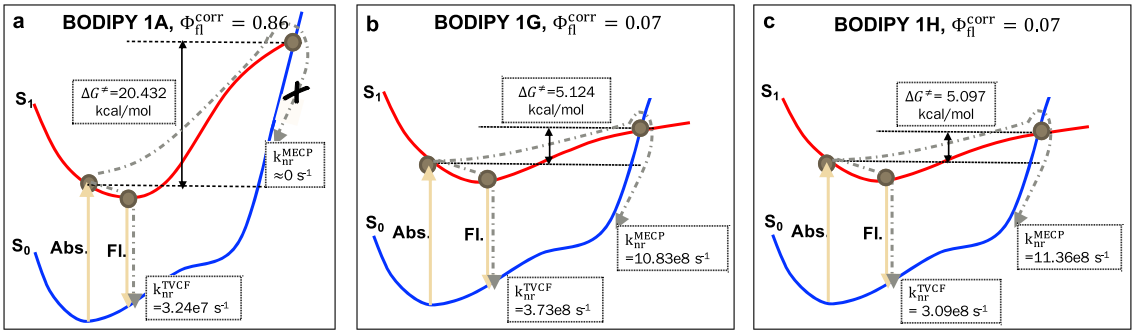

Figure 6. Schematic graph of the two nonradiative decay channels for BODIPYs (a) **1A**, (b) **1G**, and (c) **1H**. The Gibbs free energy of activation, the nonradiative decay rate constants via two channels, and the corrected quantum efficiency (Φ_{fl}^{corr}) for each molecule are listed for reference.

investigate the influence of channel II in different systems, we also perform the same calculation of k_{nr}^{MECP} for **1A**. k_{nr}^{MECP} is evaluated via TST (Eyring equation) as[63]

$$k_{nr}^{MECP} = \frac{k_B T}{h} \exp\left(-\frac{\Delta G^{\ddagger}}{RT}\right) \quad (7)$$

where $\Delta G^{\ddagger}$ is the Gibbs free energy of activation between the Franck−Condon (FC) structure and the MECP structure because no high-lying transition state (higher in energy than MECP) has been located for these three molecules along the reaction path. Explicit evaluation of $\Delta G^{\ddagger}$ and k_{nr}^{MECP} can be found in the Supporting Information (see Computational details and Table S8). We schematically plot the two-channel processes of these three molecules with the corresponding rate constants in Figure 6.

As shown in Table S8 and panels b and c of Figure 6, k_{nr}^{MECP} is larger than k_{nr}^{TVCF} for **1G** and **1H**, resulting a significant increase in the total k_{nr} and a decrease in quantum efficiency Φ_{fl}^{corr} = 0.07 for both **1G** and **1H**, which is now closer to experimental results, though still slightly larger. The remaining deviation in Φ_{fl}^{corr} for **1G** and **1H** is presumably due to the fact that the Duschinsky rotation effect plays a non-negligible role in these two molecules, which has not been taken into account in this study. For **1A** (Figure 6a), k_{nr}^{MECP} is negligible due to an extremely high $\Delta G^{\ddagger}$. Given the fact that the radiative decay rate for most BODIPY molecules at room temperature is 10^7−10^9 s^{-1}, channel II can be safely neglected if $\Delta G^{\ddagger}$ is >10 kcal/mol (with a corresponding k_{nr}^{MECP} of <10^6 s^{-1}), while it plays a dominant role in nonradiative decay processes if $\Delta G^{\ddagger}$ is <6 kcal/mol (with a corresponding k_{nr}^{MECP} of >10^8 s^{-1}). In the latter case, only by adding k_{nr}^{MECP} to the total k_{nr} can one recover a reasonable Φ_{fl} compared to the experiment.

To conclude, we have investigated the electronic structure and photophysical properties of a wide range of BODIPY molecules. The electronic structure results predicted by SF-TDDFT/B3LYP/cc-pVDZ with LR-PCM are in good agreement with experimental values for both vertical excitation energies and 0−0 energies (with the MAE being ≤0.1 eV). With the electronic structure information provided by SF-TDDFT, we have successfully recovered the experimental spectra for 13 representative BODIPYs via TVCF. To accurately predict the fluorescence quantum efficiency, we have proposed a two-channel picture to describe the IC process of the S_1 state. While channel I deactivates the molecule via direct harmonic vibrational relaxation (i.e., within the TVCF framework), the second deactivation channel (channel II) takes place via a distorted S_0/S_1 MECP structure away from the harmonic region. We have demonstrated that taking channel II into account is essential in predicting the fluorescence quantum yield for low-efficiency BODIPYs, while it is negligible for high-efficiency BODIPYs that usually have an energetically inaccessible S_0/S_1 MECP. Given the large time scale (nanoseconds) of the deactivation processes in most organic fluorescence materials, which is quite challenging to describe with nonadiabatic quantum dynamics, this two-channel scheme and the corresponding computational method we have presented in this work can serve as a practical alternative to quantum dynamics methods and a rational guideline for quantitatively predicting the Φ_{fl} for ubiquitous organic fluorescent molecules.

■ ASSOCIATED CONTENT

Supporting Information

The Supporting Information is available free of charge at https://pubs.acs.org/doi/10.1021/acs.jpclett.0c02054.

Computational details for electronic structure and rate constant calculation; explicit theoretical and experimental results for vertical excitation energies, optimized ground state geometries, and 0−0 excitation energies of investigated BODIPYs; S_1 and T_1 transition characters and energy gaps predicted by SF-TDDFT/B3LYP/cc-pVDZ with LR-PCM; additional theoretical spectra and mode-specific reorganization energies; visualized S_0, S_1, and S_0/S_1 MECP structures and relative energies of **1G** and **1H**; and Cartesian coordinates of S_0- and S_1-optimized structures for 13 representative BODIPYs (PDF)

■ AUTHOR INFORMATION

Corresponding Author

Zhigang Shuai − *MOE Key Laboratory of Organic OptoElectronics and Molecular Engineering, Department of Chemistry, Tsinghua University, Beijing 100084, China;* orcid.org/0000-0003-3867-2331; Email: zgshuai@tsinghua.edu.cn

Authors

Qi Ou − *MOE Key Laboratory of Organic OptoElectronics and Molecular Engineering, Department of Chemistry, Tsinghua University, Beijing 100084, China;* orcid.org/0000-0002-6400-7522

Qian Peng − *CAS Key Laboratory of Organic Solids, Institute of Chemistry of the Chinese Academy of Sciences, Beijing 100190, China;* orcid.org/0000-0001-8975-8413

https://dx.doi.org/10.1021/acs.jpclett.0c02054
J. Phys. Chem. Lett. 2020, 11, 7790−7797

Complete contact information is available at:
https://pubs.acs.org/10.1021/acs.jpclett.0c02054

Notes

The authors declare no competing financial interest.

■ ACKNOWLEDGMENTS

This work was supported by the National Natural Science Foundation of China through Project "Science CEnter for Luminescence from Molecular Aggregates (SCELMA)," Grant 21788102, and by the Ministry of Science and Technology of China through the National Key R&D Plan, Grant 2017YFA0204501. Q.O. thanks Dr. Zhou Lin for inspiring discussions. Q.O. is also supported by the Shuimu Tsinghua Scholar Program.

■ REFERENCES

(1) Lu, H.; Mack, J.; Yang, Y.; Shen, Z. Structural Modification Strategies for the Rational Design of Red/NIR Region BODIPYs. *Chem. Soc. Rev.* **2014**, *43*, 4778−4823.
(2) Huang, L.; Li, Z.; Zhao, Y.; Zhang, Y.; Wu, S.; Zhao, J.; Han, G. Ultralow-Power Near Infrared Lamp Light Operable Targeted Organic Nanoparticle Photodynamic Therapy. *J. Am. Chem. Soc.* **2016**, *138*, 14586−14591.
(3) Ge, Y.; O'Shea, D. F. Azadipyrromethenes: From Traditional Dye Chemistry to Leading Edge Applications. *Chem. Soc. Rev.* **2016**, *45*, 3846−3864.
(4) Jiang, M.; Gu, X.; Lam, J. W. Y.; Zhang, Y.; Kwok, R. T. K.; Wong, K. S.; Tang, B. Z. Two-Photon AIE Bio-Probe with Large Stokes Shift for Specific Imaging of Lipid Droplets. *Chem. Sci.* **2017**, *8*, 5440−5446.
(5) He, H.; Ji, S.; He, Y.; Zhu, A.; Zou, Y.; Deng, Y.; Ke, H.; Yang, H.; Zhao, Y.; Guo, Z.; Chen, H. Photoconversion-Tunable Fluorophore Vesicles for Wavelength-Dependent Photoinduced Cancer Therapy. *Adv. Mater.* **2017**, *29*, 1606690.
(6) Kim, D.; Lee, U.; Bouffard, J.; Kim, Y. Glycosaminoglycan-Induced Emissive J-Aggregate Formation in a *Meso* -Ester BODIPY Dye. *Adv. Opt. Mater.* **2020**, *8*, 1902161.
(7) Maeda, C.; Nagahata, K.; Shirakawa, T.; Ema, T. Azahelicene-Fused BODIPY Analogues Showing Circularly Polarized Luminescence. *Angew. Chem., Int. Ed.* **2020**, *59*, 7813−7817.
(8) Chen, Y.; Zhang, W.; Cai, Y.; Kwok, R. T. K.; Hu, Y.; Lam, J. W. Y.; Gu, X.; He, Z.; Zhao, Z.; Zheng, X.; et al. AIEgens for Dark Through-Bond Energy Transfer: Design, Synthesis, Theoretical Study and Application in Ratiometric Hg^{2+} Sensing. *Chem. Sci.* **2017**, *8*, 2047−2055.
(9) Mazzone, G.; Quartarolo, A. D.; Russo, N. PDT-Correlated Photophysical Properties of Thienopyrrole BODIPY Derivatives. Theoretical Insights. *Dyes Pigm.* **2016**, *130*, 9−15.
(10) Momeni, M. R.; Brown, A. A Local CC2 and TDA-DFT Double Hybrid Study on BODIPY/Aza-BODIPY Dimers as Heavy Atom Free Triplet Photosensitizers for Photodynamic Therapy Applications. *J. Phys. Chem. A* **2016**, *120*, 2550−2560.
(11) Lin, Z.; Kohn, A. W.; Van Voorhis, T. Toward Prediction of Nonradiative Decay Pathways in Organic Compounds II: Two Internal Conversion Channels in BODIPYs. *J. Phys. Chem. C* **2020**, *124*, 3925−3938.
(12) Chibani, S.; Le Guennic, B.; Charaf-Eddin, A.; Laurent, A. D.; Jacquemin, D. Revisiting the Optical Signatures of BODIPY with Ab Initio Tools. *Chem. Sci.* **2013**, *4*, 1950−1963.
(13) Jacquemin, D.; Adamo, C. Computational Molecular Electronic Spectroscopy with TD-DFT. In *Density-Functional Methods for Excited States*; Ferré, N., Filatov, M., Huix-Rotllant, M., Eds.; Topics in Current Chemistry; Springer International Publishing: Cham, Switzerland, 2015; Vol. *368*, pp 347−375.
(14) Momeni, M. R.; Brown, A. Why Do TD-DFT Excitation Energies of BODIPY/Aza-BODIPY Families Largely Deviate from Experiment? Answers from Electron Correlated and Multireference Methods. *J. Chem. Theory Comput.* **2015**, *11*, 2619−2632.
(15) de Jong, F.; Feldt, M.; Feldt, J.; Harvey, J. N. Modelling Absorption and Emission of a *Meso* -Aniline-BODIPY Based Dye with Molecular Mechanics. *Phys. Chem. Chem. Phys.* **2018**, *20*, 14537−14544.
(16) Dura, L.; Wächtler, M.; Kupfer, S.; Kübel, J.; Ahrens, J.; Höfler, S.; Bröring, M.; Dietzek, B.; Beweries, T. Photophysics of BODIPY Dyes as Readily-Designable Photosensitisers in Light-Driven Proton Reduction. *Inorganics* **2017**, *5*, 21.
(17) Chibani, S.; Laurent, A. D.; Le Guennic, B.; Jacquemin, D. Improving the Accuracy of Excited-State Simulations of BODIPY and Aza-BODIPY Dyes with a Joint SOS-CIS(D) and TD-DFT Approach. *J. Chem. Theory Comput.* **2014**, *10*, 4574−4582.
(18) Koch, A.; Kinzel, D.; Dröge, F.; Gräfe, S.; Kupfer, S. Photochemistry and Electron Transfer Kinetics in a Photocatalyst Model Assessed by Marcus Theory and Quantum Dynamics. *J. Phys. Chem. C* **2017**, *121*, 16066−16078.
(19) Menger, M. F. S. J.; Plasser, F.; Mennucci, B.; González, L. Surface Hopping within an Exciton Picture. An Electrostatic Embedding Scheme. *J. Chem. Theory Comput.* **2018**, *14*, 6139−6148.
(20) Westermayr, J.; Gastegger, M.; Menger, M. F. S. J.; Mai, S.; González, L.; Marquetand, P. Machine Learning Enables Long Time Scale Molecular Photodynamics Simulations. *Chem. Sci.* **2019**, *10*, 8100−8107.
(21) Shuai, Z.; Peng, Q. Excited States Structure and Processes: Understanding Organic Light-Emitting Diodes at the Molecular Level. *Phys. Rep.* **2014**, *537*, 123−156.
(22) Shuai, Z.; Peng, Q. Organic Light-Emitting Diodes: Theoretical Understanding of Highly Efficient Materials and Development of Computational Methodology. *Natl. Sci. Rev.* **2017**, *4*, 224−239.
(23) Petrushenko, I. K.; Petrushenko, K. B. Effect of Meso-Substituents on the Electronic Transitions of BODIPY Dyes: DFT and RI-CC2 Study. *Spectrochim. Acta, Part A* **2015**, *138*, 623−627.
(24) Valiev, R. R.; Sinelnikov, A. N.; Aksenova, Y. V.; Kuznetsova, R. T.; Berezin, M. B.; Semeikin, A. S.; Cherepanov, V. N. The Computational and Experimental Investigations of Photophysical and Spectroscopic Properties of BF2 Dipyrromethene Complexes. *Spectrochim. Acta, Part A* **2014**, *117*, 323−329.
(25) Briggs, E. A.; Besley, N. A.; Robinson, D. QM/MM Excited State Molecular Dynamics and Fluorescence Spectroscopy of BODIPY. *J. Phys. Chem. A* **2013**, *117*, 2644−2650.
(26) Jiao, L.; Yu, C.; Wang, J.; Briggs, E. A.; Besley, N. A.; Robinson, D.; Ruedas-Rama, M. J.; Orte, A.; Crovetto, L.; Talavera, E. M.; et al. Unusual Spectroscopic and Photophysical Properties of Meso-Tert-ButylBODIPY in Comparison to Related Alkylated BODIPY Dyes. *RSC Adv.* **2015**, *5*, 89375−89388.
(27) Duman, S.; Cakmak, Y.; Kolemen, S.; Akkaya, E. U.; Dede, Y. Heavy Atom Free Singlet Oxygen Generation: Doubly Substituted Configurations Dominate S_1 States of Bis-BODIPYs. *J. Org. Chem.* **2012**, *77*, 4516−4527.
(28) Wen, J.; Han, B.; Havlas, Z.; Michl, J. An MS-CASPT2 Calculation of the Excited Electronic States of an Axial Difluoroboron-dipyrromethene (BODIPY) Dimer. *J. Chem. Theory Comput.* **2018**, *14*, 4291−4297.
(29) Ziems, K.; Gräfe, S.; Kupfer, S. Photo-Induced Charge Separation vs. Degradation of a BODIPY-Based Photosensitizer Assessed by TDDFT and RASPT2. *Catalysts* **2018**, *8*, 520.
(30) De Vetta, M.; González, L.; Corral, I. The Role of Electronic Triplet States and High-Lying Singlet States in the Deactivation Mechanism of the Parent BODIPY: An ADC(2) and CASPT2 Study. *ChemPhotoChem.* **2019**, *3*, 727−738.
(31) Matulis, V. E.; Ragoyja, E. G.; Ivashkevich, O. A. Accurate Theoretical Prediction of Optical Properties of BODIPY Dyes. *Int. J. Quantum Chem.* **2020**, *120*, 120.
(32) Laine, M.; Barbosa, N. A.; Wieczorek, R.; Melnikov, M. Ya.; Filarowski, A. Calculations of BODIPY Dyes in the Ground and Excited States Using the M06-2X and PBE0 Functionals. *J. Mol. Model.* **2016**, *22*, 260.

(33) Mallah, R.; Sreenath, M. C.; Chitrambalam, S.; Joe, I. H.; Sekar, N. Excitation Energy Transfer Processes in BODIPY Based Donor-Acceptor System - Synthesis, Photophysics, NLO and DFT Study. *Opt. Mater.* **2018**, *84*, 795−806.
(34) Shao, Y.; Head-Gordon, M.; Krylov, A. I. The Spin-Flip Approach within Time-Dependent Density Functional Theory: Theory and Applications to Diradicals. *J. Chem. Phys.* **2003**, *118*, 4807−4818.
(35) Shao, Y.; Gan, Z.; Epifanovsky, E.; Gilbert, A. T. B.; Wormit, M.; Kussmann, J.; Lange, A. W.; Behn, A.; Deng, J.; Feng, X.; et al. Advances in Molecular Quantum Chemistry Contained in the Q-Chem 4 Program Package. *Mol. Phys.* **2015**, *113*, 184−215.
(36) Miertuš, S.; Scrocco, E.; Tomasi, J. Electrostatic Interaction of a Solute with a Continuum. A Direct Utilizaion of AB Initio Molecular Potentials for the Prevision of Solvent Effects. *Chem. Phys.* **1981**, *55*, 117−129.
(37) Cammi, R.; Mennucci, B. Linear Response Theory for the Polarizable Continuum Model. *J. Chem. Phys.* **1999**, *110*, 9877−9886.
(38) Cossi, M.; Barone, V. Time-Dependent Density Functional Theory for Molecules in Liquid Solutions. *J. Chem. Phys.* **2001**, *115*, 4708−4717.
(39) Bernard, Y. A.; Shao, Y.; Krylov, A. I. General Formulation of Spin-Flip Time-Dependent Density Functional Theory Using Non-Collinear Kernels: Theory, Implementation, and Benchmarks. *J. Chem. Phys.* **2012**, *136*, 204103.
(40) Lasorne, B.; Jornet-Somoza, J.; Meyer, H.-D.; Lauvergnat, D.; Robb, M. A.; Gatti, F. Vertical Transition Energies vs. Absorption Maxima: Illustration with the UV Absorption Spectrum of Ethylene. *Spectrochim. Acta, Part A* **2014**, *119*, 52−58.
(41) Jacquemin, D.; Perpète, E. A.; Vydrov, O. A.; Scuseria, G. E.; Adamo, C. Assessment of Long-Range Corrected Functionals Performance for N→π^* Transitions in Organic Dyes. *J. Chem. Phys.* **2007**, *127*, 094102.
(42) Jacquemin, D.; Perpète, E. A.; Scuseria, G. E.; Ciofini, I.; Adamo, C. TD-DFT Performance for the Visible Absorption Spectra of Organic Dyes: Conventional versus Long-Range Hybrids. *J. Chem. Theory Comput.* **2008**, *4*, 123−135.
(43) Jacquemin, D.; Wathelet, V.; Perpète, E. A.; Adamo, C. Extensive TD-DFT Benchmark: Singlet-Excited States of Organic Molecules. *J. Chem. Theory Comput.* **2009**, *5*, 2420−2435.
(44) Goerigk, L.; Grimme, S. Assessment of TD-DFT Methods and of Various Spin Scaled CIS(D) and CC2 Versions for the Treatment of Low-Lying Valence Excitations of Large Organic Dyes. *J. Chem. Phys.* **2010**, *132*, 184103.
(45) Send, R.; Kühn, M.; Furche, F. Assessing Excited State Methods by Adiabatic Excitation Energies. *J. Chem. Theory Comput.* **2011**, *7*, 2376−2386.
(46) Jacquemin, D.; Planchat, A.; Adamo, C.; Mennucci, B. TD-DFT Assessment of Functionals for Optical 0−0 Transitions in Solvated Dyes. *J. Chem. Theory Comput.* **2012**, *8*, 2359−2372.
(47) Peng, Q.; Yi, Y.; Shuai, Z.; Shao, J. Toward Quantitative Prediction of Molecular Fluorescence Quantum Efficiency: Role of Duschinsky Rotation. *J. Am. Chem. Soc.* **2007**, *129*, 9333−9339.
(48) Shuai, Z. Thermal Vibration Correlation Function Formalism for Molecular Excited State Decay Rates. *Chin. J. Chem.* **2020**, *38*, 1223−1232.
(49) Niu, Y.; Peng, Q.; Deng, C.; Gao, X.; Shuai, Z. Theory of Excited State Decays and Optical Spectra: Application to Polyatomic Molecules. *J. Phys. Chem. A* **2010**, *114*, 7817−7831.
(50) Zhang, X.-F.; Zhu, J. BODIPY Parent Compound: Fluorescence, Singlet Oxygen Formation and Properties Revealed by DFT Calculations. *J. Lumin.* **2019**, *205*, 148−157.
(51) Zhou, Y.; Xiao, Y.; Li, D.; Fu, M.; Qian, X. Novel Fluorescent Fluorine-Boron Complexes: Synthesis, Crystal Structure, Photoluminescence, and Electrochemistry Properties. *J. Org. Chem.* **2008**, *73*, 1571−1574.
(52) El-Sayed, M. A. Triplet State. Its Radiative and Nonradiative Properties. *Acc. Chem. Res.* **1968**, *1*, 8−16.
(53) Prlj, A.; Vannay, L.; Corminboeuf, C. Fluorescence Quenching in BODIPY Dyes: The Role of Intramolecular Interactions and Charge Transfer. *Helv. Chim. Acta* **2017**, *100*, No. e1700093.
(54) Pavlopoulos, T. G.; Boyer, J. H.; Shah, M.; Thangaraj, K.; Soong, M.-L. Laser Action from 2,6,8-Position Trisubstituted 1,3,5,7-Tetramethylpyrromethene-BF_2 Complexes: Part 1. *Appl. Opt.* **1990**, *29*, 3885.
(55) Bañuelos, J.; Martín, V.; Gómez-Durán, C. F. A.; Córdoba, I. J. A.; Peña-Cabrera, E.; García-Moreno, I.; Costela, Á.; Pérez-Ojeda, M. E.; Arbeloa, T.; Arbeloa, Í. L. New 8-Amino-BODIPY Derivatives: Surpassing Laser Dyes at Blue-Edge Wavelengths. *Chem. - Eur. J.* **2011**, *17*, 7261−7270.
(56) Arroyo, I. J.; Hu, R.; Tang, B. Z.; López, F. I.; Peña-Cabrera, E. 8-Alkenylborondipyrromethene Dyes. General Synthesis, Optical Properties, and Preliminary Study of Their Reactivity. *Tetrahedron* **2011**, *67*, 7244−7250.
(57) Yu, C.; Jiao, L.; Yin, H.; Zhou, J.; Pang, W.; Wu, Y.; Wang, Z.; Yang, G.; Hao, E. α-/β-Formylated Boron-Dipyrrin (BODIPY) Dyes: Regioselective Syntheses and Photophysical Properties. *Eur. J. Org. Chem.* **2011**, *2011*, 5460−5468.
(58) Jiao, L.; Yu, C.; Liu, M.; Wu, Y.; Cong, K.; Meng, T.; Wang, Y.; Hao, E. Synthesis and Functionalization of Asymmetrical Benzo-Fused BODIPY Dyes. *J. Org. Chem.* **2010**, *75*, 6035−6038.
(59) Umezawa, K.; Nakamura, Y.; Makino, H.; Citterio, D.; Suzuki, K. Bright, Color-Tunable Fluorescent Dyes in the Visible-Near-Infrared Region. *J. Am. Chem. Soc.* **2008**, *130*, 1550−1551.
(60) Jiang, X.-D.; Zhang, H.; Zhang, Y.; Zhao, W. Development of Non-Symmetric Thiophene-Fused BODIPYs. *Tetrahedron* **2012**, *68*, 9795−9801.
(61) Kubota, Y.; Hara, H.; Tanaka, S.; Funabiki, K.; Matsui, M. Synthesis and Fluorescence Properties of Novel Pyrazine-Boron Complexes Bearing a β-Iminoketone Ligand. *Org. Lett.* **2011**, *13*, 6544−6547.
(62) Levine, B. G.; Coe, J. D.; Martínez, T. J. Optimizing Conical Intersections without Derivative Coupling Vectors: Application to Multistate Multireference Second-Order Perturbation Theory (MS-CASPT2). *J. Phys. Chem. B* **2008**, *112*, 405−413.
(63) Laidler, K. J.; Meiser, J. H. *Physical Chemistry*; Benjamin/Cummings Publishing Co.: Menlo Park, CA, 1982.

https://dx.doi.org/10.1021/acs.jpclett.0c02054
J. Phys. Chem. Lett. 2020, 11, 7790−7797